Supporting information

Tunable Plasmonic Microcapsules with Embedded Noble Metal Nanoparticles for Optical Microsensing

*Céline Burel[1], Omar Ibrahim[2], Emanuele Marino[2], Harshit Bharti[3], Christopher B. Murray[2,3], Bertrand Donnio[4], Zahra Fakhraai[2], Rémi Dreyfus[1,5]**

[1]Complex Assemblies of Soft Matter Laboratory (COMPASS), UMI 3254, CNRS-Solvay-University of Pennsylvania, CRTB, Bristol, PA 19007, United States
E-mail: remi.dreyfus@cnrs.fr
[2]Dept of Chemistry, University of Pennsylvania, 231 S. 34th Street, Philadelphia, PA 19104, USA
[3]Dept of Materials Science and Engineering, University of Pennsylvania, 231 S. 34th Street, Philadelphia, PA 19104, USA
[4]Institut de Physique et Chimie des Matériaux de Strasbourg (IPCMS), UMR 7504, CNRS-Université de Strasbourg, 67034, Strasbourg, France
[5]Laboratoire Nanotechnologies Nanosystèmes (LN2), CNRS - Université de Sherbrooke 3000 Boulevard de l'Université, Sherbrooke, Qc, J1K 0A5, Canada

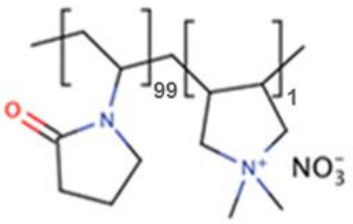

Figure S1. Chemical structure of PVP-DADMAN® (99:1). PVP-DADMAN® contains 1 unit of diallyldimethylammonium-nitrate (DADMAN) for 99 units of Polyvinylpyrrolidone (PVP) (Mw = 60 kg/mol, pKa = 5).

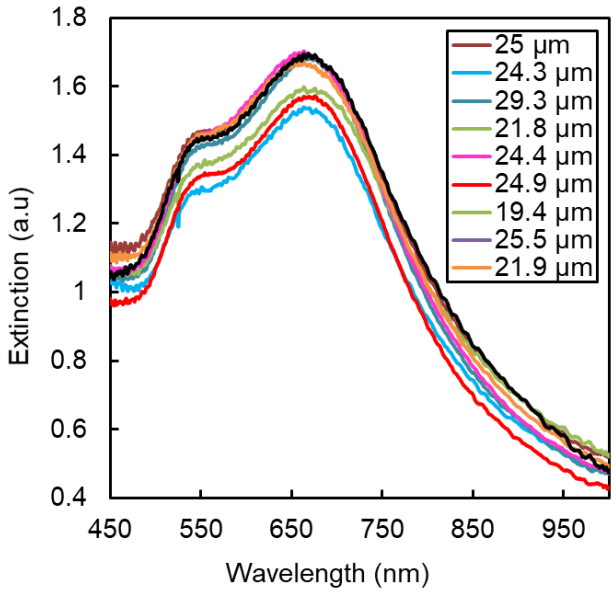

Figure S2. Extinction of blue Au Si MCs of different sizes containing toluene and dispersed in water.

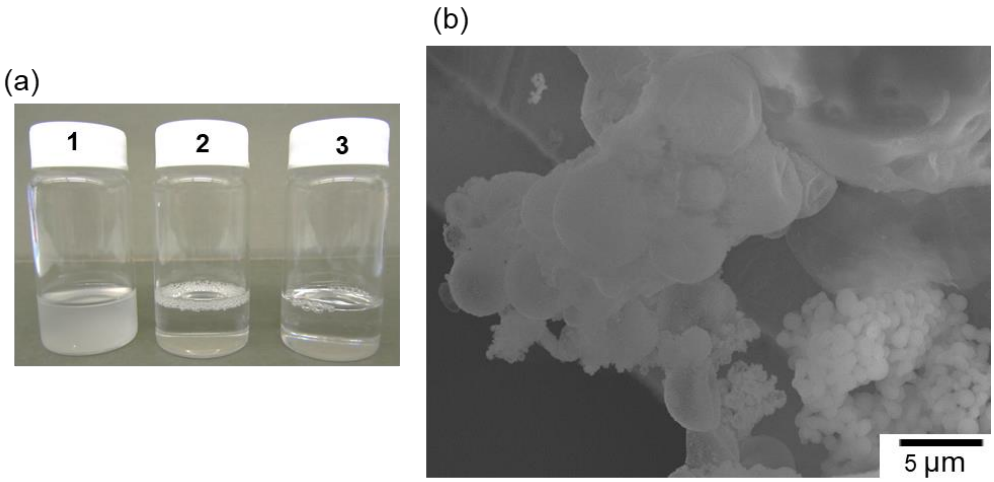

Figure S3. (a) PEOS mixed with hexadecane (1), toluene (2) and a 50/50 v/v mixture of hexadecane/hexyl/acetate(3). (b) SEM image of Au MCs obtained with 0.2g PEOS in hexadecane.

Optical simulations

Two different sets of simulations were performed: one based directly on experimental packings ("SEM packings") and one based on simulated packings ("DCCP packings") with structural parameters based on experimental packings.

For the SEM packings, NPs edges were manually identified, and, assuming NPs were perfectly spherical, we were able to reconstruct a packing of NPs. A small subset of the reconstructed packing of NPs was made periodic and any overlapping beads (by minimum image convention) were removed. Simulations were then performed at various inter-bead distances (which had the same packings and bead sizes, but with all the bead positions scaled) and performed with and without the silica slab and with either air on each side or water/toluene on either side (Figure S5). The extinction coefficient for each geometry was calculated based on the simulated transmission coefficient. Figures S6 and S7 shows the result of these simulations. We see that in the case of both Ag and Au NPs we have an absorption peak that remains approximately fixed corresponding to the single particle absorption. However, as we pack the particles closer together, we also see a rise in additional peaks resulting from plasmon coupling between the beads. This coupling is enhanced in higher-index materials as seen in the case of beads embedded in silica or suspended in the water/toluene instead of air.

For the DCCP packings, SEM images of Ag and Au nanoparticles were also used. The size distribution of Ag and Au NPs was measured by fitting the contour of each NP on the SEM image. The obtained size distributions were further fitted by lognormal distributions to extract the parameters σ and μ of the lognormal distribution for the NPs radii $p(R) = \frac{1}{\sigma R\sqrt{2\pi}} e^{\left(-\frac{(\ln(R)-\mu)^2}{2\sigma^2}\right)}$ where R is the NP radius in nm. The fitted parameters σ and μ are respectively 2.8114 and 0.3894 for Au NPs and 2.6813 and 0.4272 for Ag NPs. To create packings of 200 particles, we randomly pick 200*x* values of radius in the Ag lognormal distribution and 200(1-*x*) values of radii in the Au lognormal distributions, where *x* is the number fraction of Ag NPs. To each values of Au NP radii, 0.25 nm in added while 8 nm is added to each value of Ag NP radii to account for the PVP-DADMAN® adsorbed at the surface. These values are extracted from the pair correlation curves shown in the main article. We then used the DCCP software [1] to generate random close packings from the 200 particles by treating them as hard spheres. Examples of four packings are provided in figure 1 for $x = 0$ (pure Au NPs), $x = 0.4$ (40% Ag NPs), $x = 0.66$ (66% Ag NPs) and $x = 1$ (100% Ag NPs).

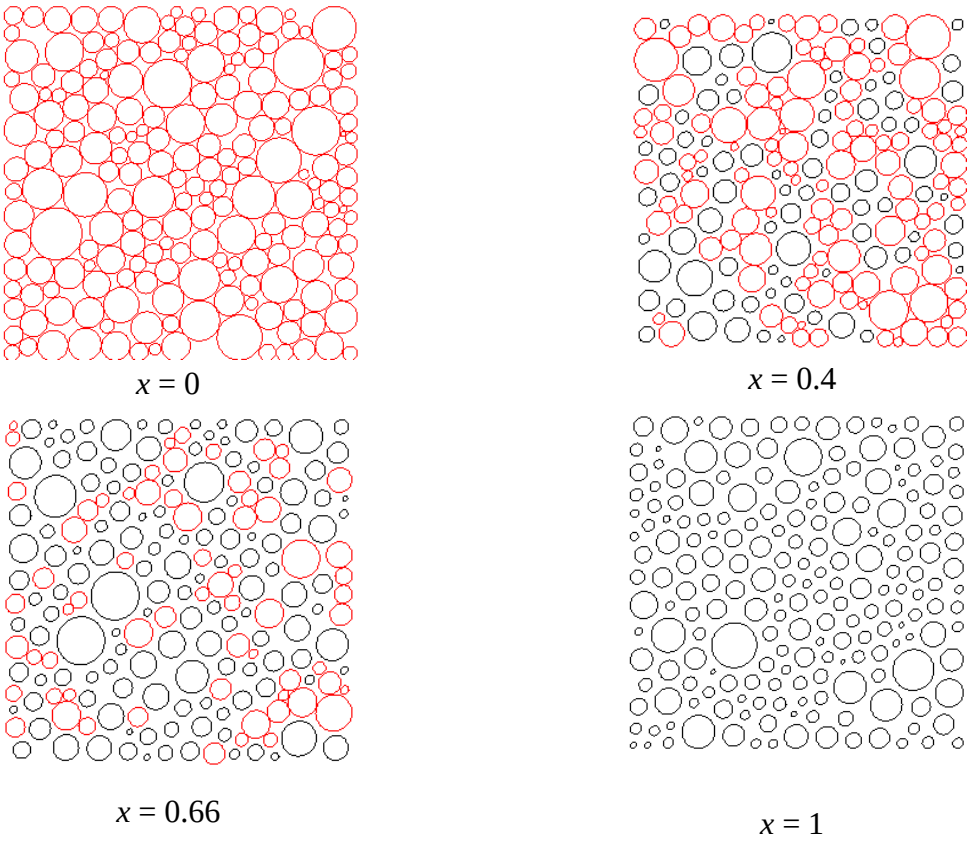

Figure S4. Simulated packing for mixtures of Au (red) and Ag (grey) NPs. *x* is the number fraction of Ag NPs.

The structures were then imported into the Lumerical FDTD Solutions package. The NPs were embedded at the center of a 60 nm thick silica slab (Figure S5 b&d). Particles that were larger than the layer had a 3 nm silica coating applied, to ensure that they are engulfed in silica, as is the case in the experiments. The optical properties used for Au and Ag beads are based on those in the CRC Handbook of Chemistry and Physics [2]. Periodic boundary conditions were applied in the *xy* direction to give an infinite slab modeling the large microcapsules and a perfectly matched layer (PML) was applied on either side of the slab in the negative and positive *z* direction (outside of the regions shown in Figure 5 c&d) to absorb the outgoing radiation. A plane wave was injected normal to the slab and the transmission coefficient was computed via a monitor placed on the other side. The simulation region was made 1.5 μm long in the z direction to ensure that the PML was far from the transmission monitor and the silica-bead region, to avoid potential backscattering. Note that these simulations used a mesh size of 2 nm.

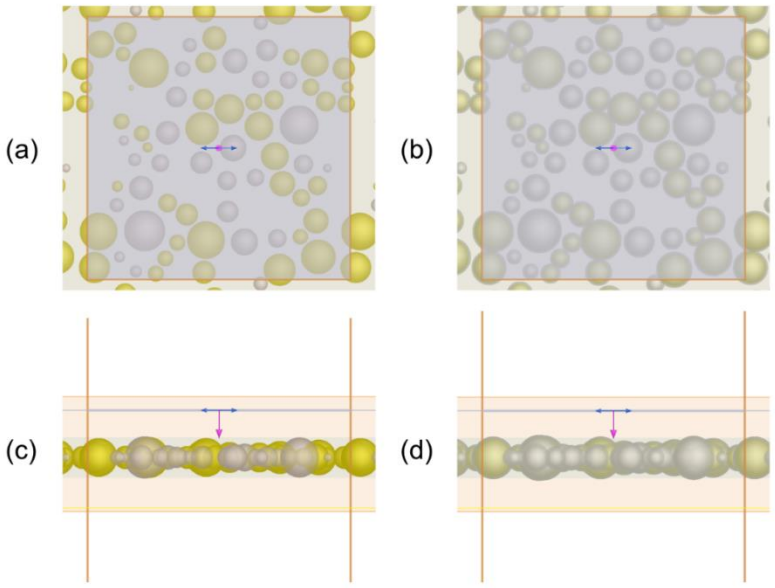

Figure S5. FDTD simulation region for sample microcapsule simulations. We show: (a) an *xy*-plane view of the region, (b) an *xy*-plane view of the region with silica shells coating the NPs, (c) an *xz*-plane view of the region, and (d) an *xz*-plane view of the region with silica shells coating the NPs. As can be seen, the silica shells help prevent the NPs from poking through the silica layer. The orange box in the (a) and (b) view represents the simulation region and PBCs are defined on this boundary. The region shaded in orange in the (c) and (d) view represents the mesh region with the PBC boundaries indicated by the vertical orange lines. The grey horizontal line in the *xz*-plane view represents the location of the plane-wave source. The pink and blue arrows show the orientation of the propagation vector and polarization directions of the incident light, respectively. The yellow line near the bottom of the mesh region in (c) and (d) shows the transmission monitor.

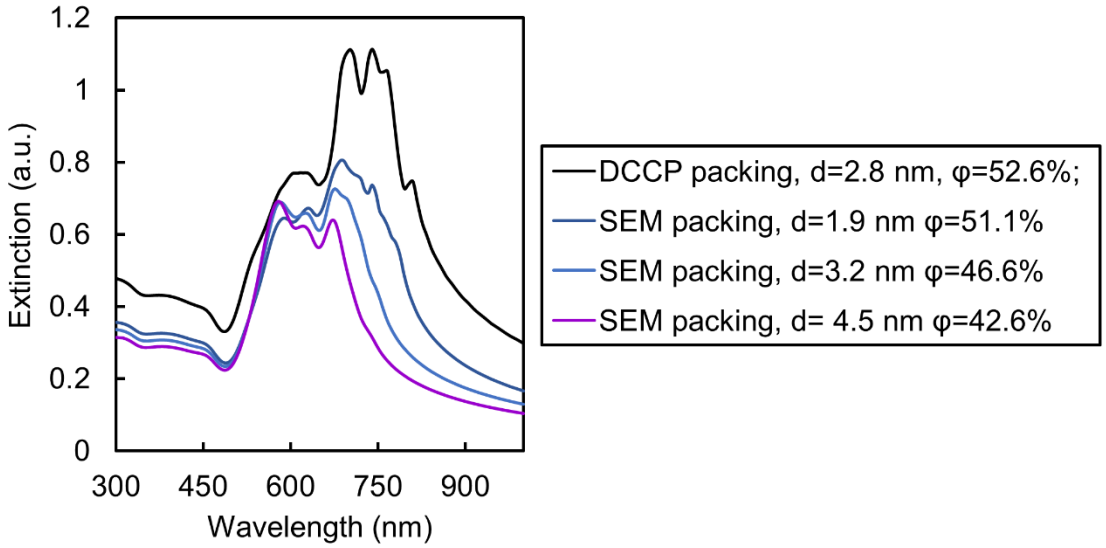

Figure S6. Comparison of SEM and DCCP simulations. The simulations were run in air above and below the Au NPs packing embedded in silica.

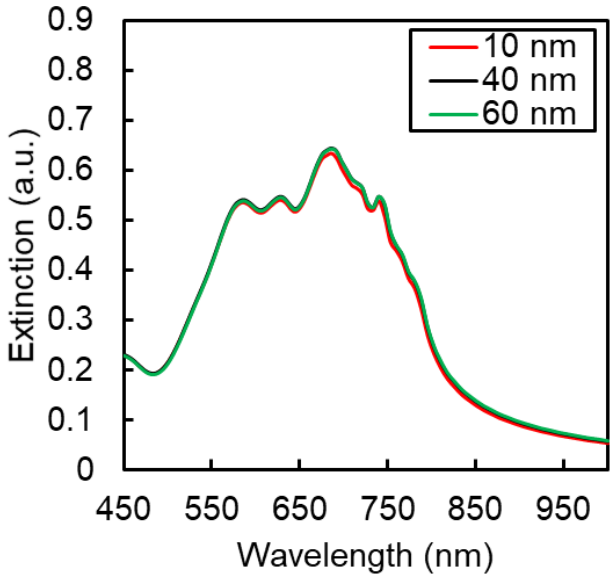

Figure S7. Impact of the silica shell thickness on the MC's extinction. The oil phase is toluene. The mean interparticle distance between Au NPs and the packing fraction are set to d=1.9 nm and φ=51.1%, respectively.

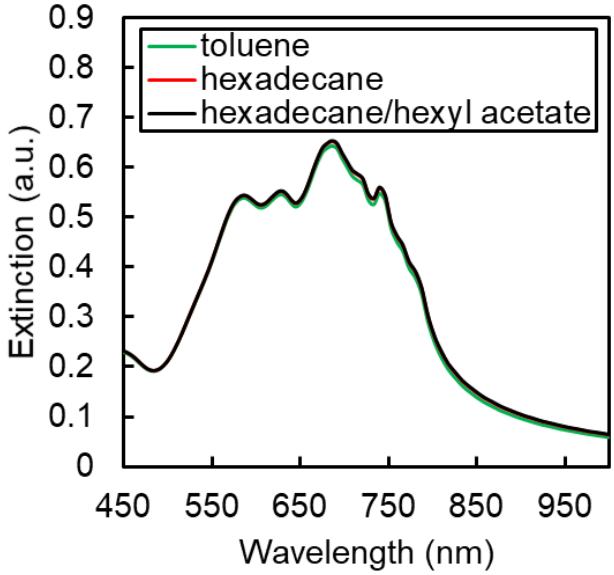

Figure S8. Impact of different oils on the MC's extinction. The silica shell thickness is set to 60 nm. The mean interparticle distance between Au NPs and the packing fraction are set to d=1.9 nm and φ=51.1%, respectively. Refractive indexes used for toluene is 1.5, hexadecane is 1.43 and hexyl acetate is 1.41.

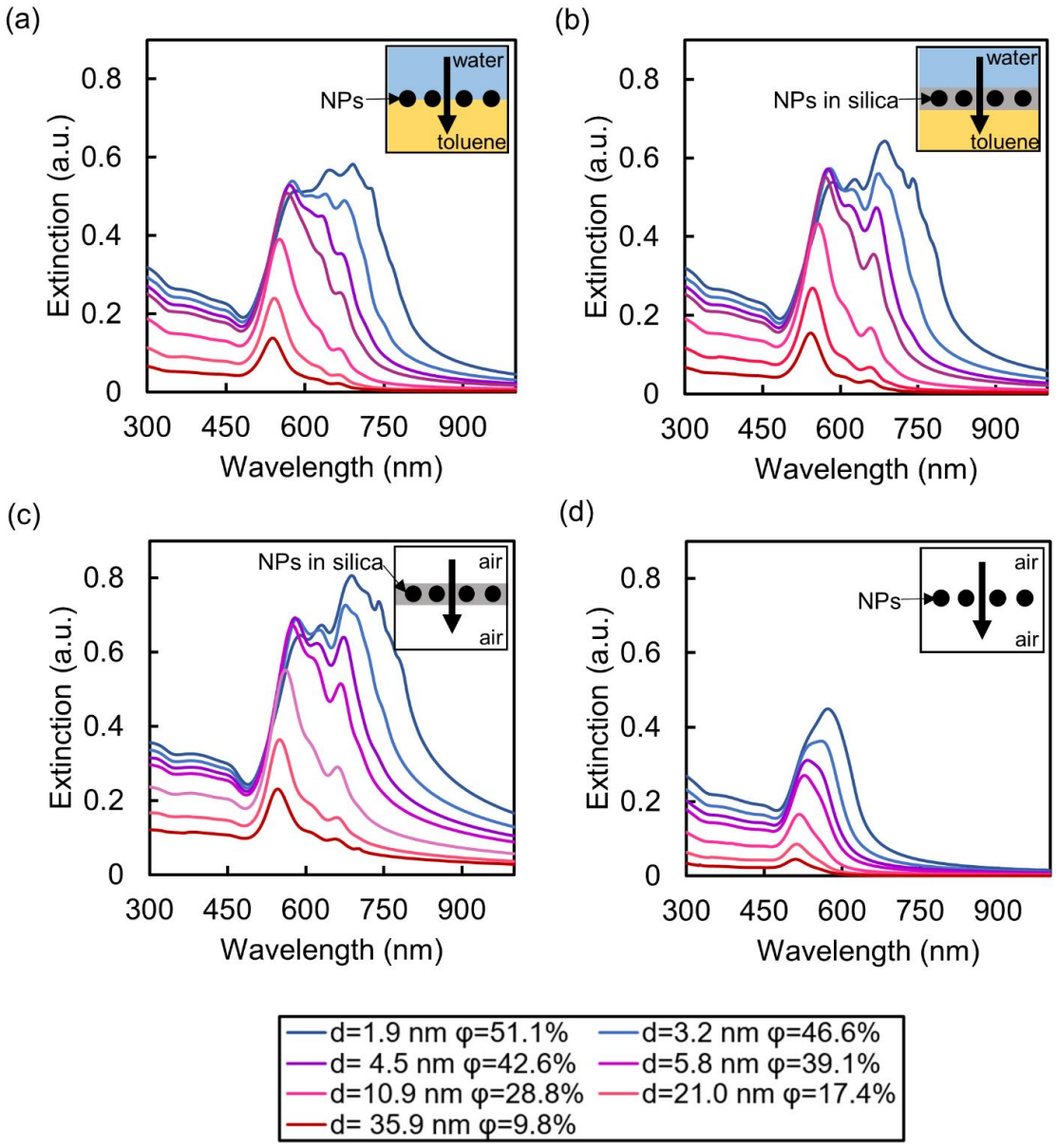

Figure S9. Simulated extinction of Au NPs (a) packed on the toluene/water droplet, (b) embedded within a silica shell at the toluene/water interface, (c) embedded within a silica shell at the toluene/water interface and then dried, (d) packed on toluene/water droplet and then dried. The insets show schematic drawings of each condition.

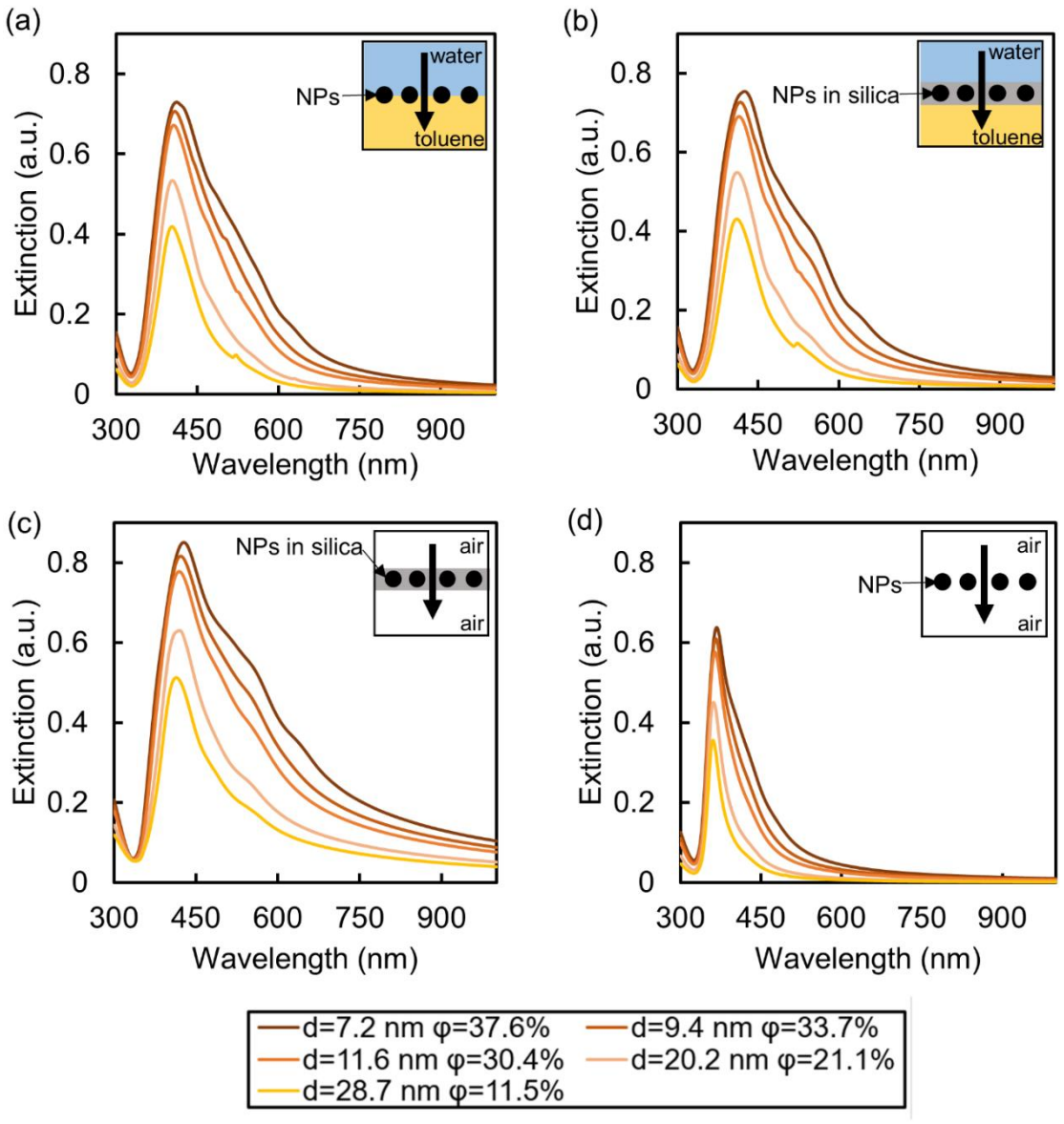

Figure S10. Simulated extinction of Ag NPs (a) packed on the toluene/water droplet, (b) embedded within a silica shell at the toluene/water interface, (c) embedded within a silica shell at the toluene/water interface and then dried, (d) packed on toluene/water droplet and then dried.

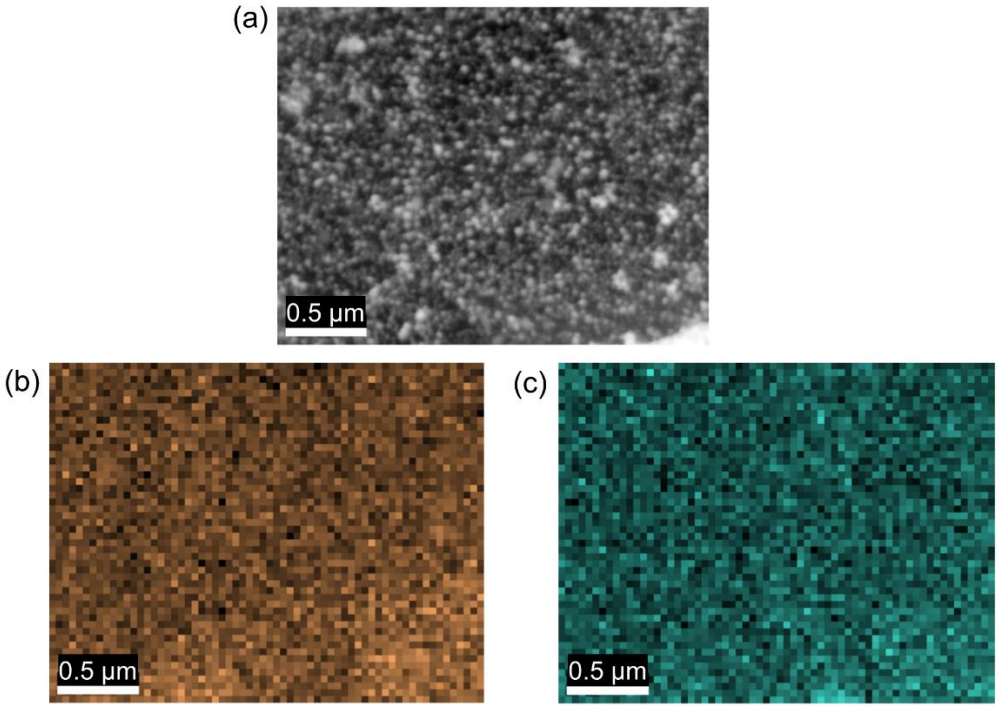

Figure S11. (a) SEM image and EDS images that illustrate the co-existence of (b) Au and (c) Ag NPs on the surface of the MCs.

SEM packings simulations could only be done for the pure Au and pure Ag NPs packings. Thus, we performed FDTD simulations on the DCCP packings in order to also obtain simulated data for Au/Ag mixtures. The procedure was very similar to above, except that the periodic region was obtained from a subset of the simulated packings shown in Figure S4. Gold bead radii were scaled by 1 nm and particles were randomly removed to match the inter particle distance and packing fraction φ of the experimental packings. The mixed packing fraction was taken to be a linear combination of the pure Au and pure Ag packing densities. We also performed these mixed simulations with only the Au beads and only the Ag beads to determine the identity of the peaks in the mixed spectra. Figure S12 shows the results of these simulations. As can be seen from this decomposition, the total spectrum has peaks resulting from the absorption of individual Au and Ag NPs as well as the plasmon coupling modes unique to the mixed system, if any. However, there is little to no apparent Au-Ag coupling as the features in the total spectrum are mostly derived from combining the two pure spectra.

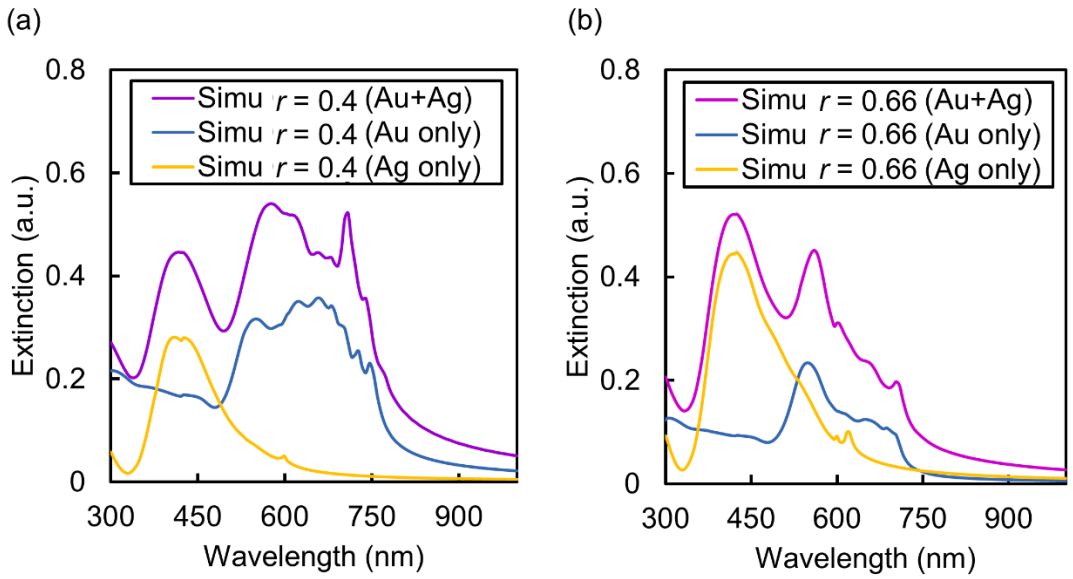

Figure S12. Simulated extinction of packing obtained with mixtures of Au and Ag NPs embedded in silica for (a) r = 0.4 and (b) r = 0.66. For both ratios, the Ag NPs or the Au NPs were removed from the packing to study independent plasmon coupling of Au and Ag NPs alone. The simulations were run in water above and toluene below the layer of NPs embedded in silica.

We have also performed simulations using monodisperse Au NPs to see if this will sharpen the response. To obtain disordered monodisperse Au NP packings, we used the mean Au particle size of 30 nm for all Au particles and distributed them using a Monte Carlo method with a hard spheres potential that penalized touching beads. Periodic boundary conditions were applied for this distribution method. The packing parameters (nearest neighbor distances and packing fraction) mimicked those of the polydisperse simulations. We did this for 3 different packings as shown in Figure S9. Overall, broad spectra are observed similar to the polydisperse case, indicating that the optical response of disordered packings of monodisperse Au NPs in MC would likely not be significantly different from the extinction observed experimentally with disordered packings of polydisperse Au NPs.

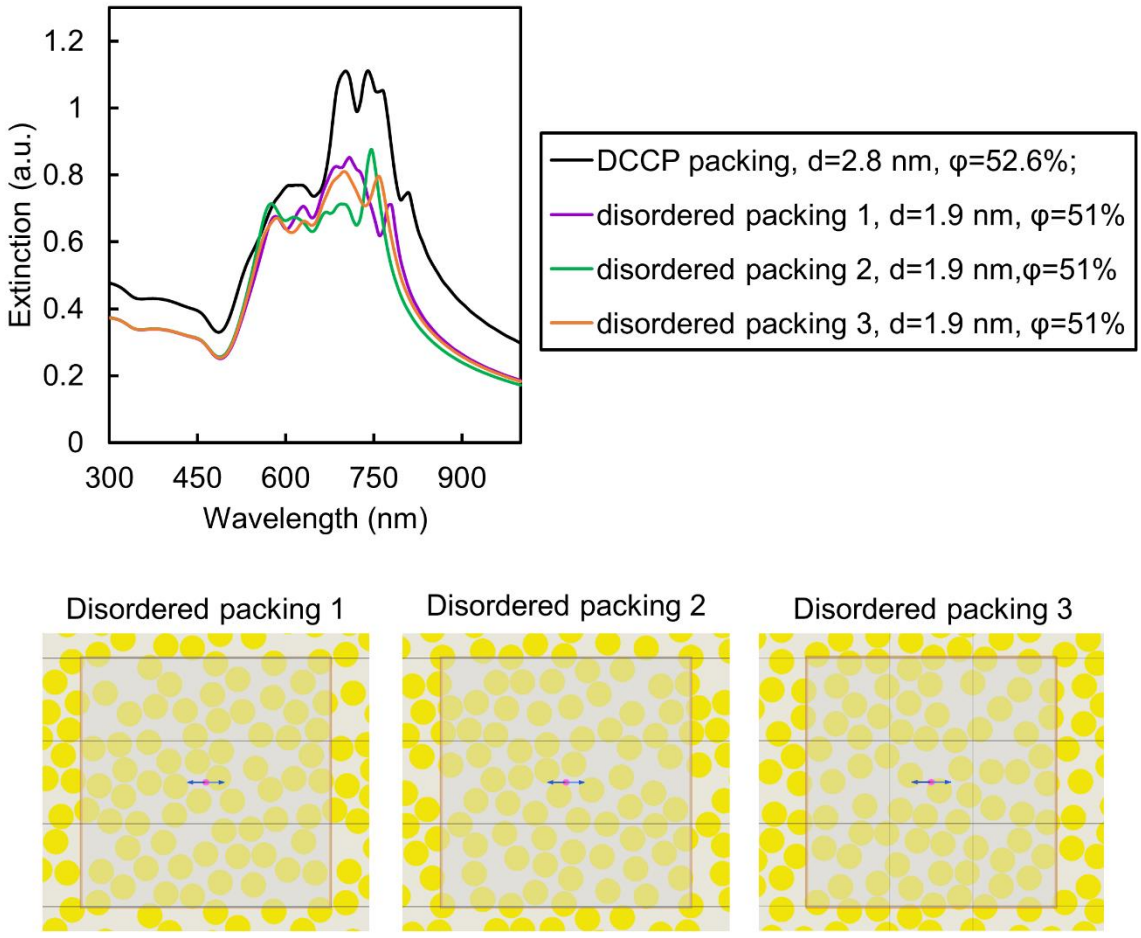

Figure S13. Simulated extinctions of 3 disordered packings of monodisperse Au NPs embedded in silica corresponding simulation images. The simulations were run in air above and below the layer of NPs embedded in silica.

We then repeated these simulations using highly ordered packings. To obtain ordered packings, we switched the Monte Carlo distribution potential to an electrostatic potential. We used similar packing parameters to the previous simulations, and we also performed simulations with a higher packing fractions for comparison. In ordered packings we see fewer features, which are also sharper in nature compared to the disordered monodisperse and polydisperse packings. This is likely due to the uniform distances between neighboring particles. However, we do still observe some broadening at higher packing fractions due to more long-range interactions between NPs. Interestingly, results presented in Figure S10 show that the extinction band of disordered packings of polydispersed Au NPs can be red-shifted because a smaller average inter-particles distance can be obtained with polydispersed Au NPs as compared to monodisperse Au NPs.

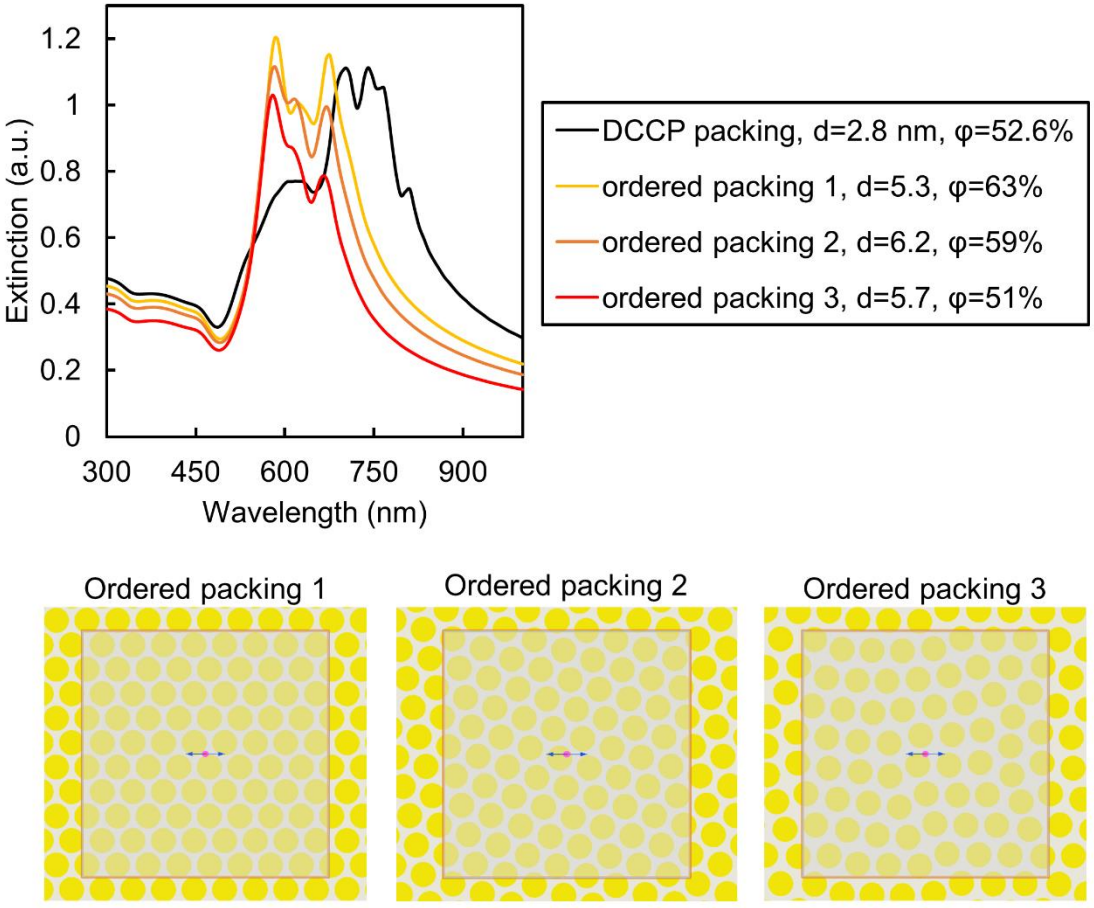

Figure S14. Simulated extinctions of 3 organized packings of monodisperse Au NPs embedded in silica corresponding simulation images. The simulations were run in air above and below the layer of NPs embedded in silica.

[1] https://github.com/cvxgrp/dccp
[2] Haynes, W. M. *CRC Handbook of Chemistry and Physics*, 95th ed.; CRC Press: USA, 2014.